Coherently wavelength injection-locking a 600-μm long cavity colorless laser diode for 16-QAM OFDM at 12 Gbit/s over 25-km SMF

Yi-Cheng Li,[1] Yu-Chieh Chi,[1] Min-Chi Cheng,[1] I-Cheng Lu,[2] Jason Chen,[2] and Gong-Ru Lin[1,*]

[1]*Graduate Institute of Photonics and Optoelectronics and Department of Electrical Engineering, National Taiwan University, No.1, Sec. 4, Roosevelt Road, Taipei 10617, Taiwan*
[2]*Department of Photonics, National Chiao Tung University, Hsinchu 300, Taiwan*
[*]*grlin@ntu.edu.tw*

Abstract: The coherent injection-locking and directly modulation of a long-cavity colorless laser diode with 1% end-facet reflectance and weak-resonant longitudinal modes is employed as an universal optical transmitter to demonstrated for optical 16-QAM OFDM transmission at 12 Gbit/s over 25 km in a DWDM-PON system. The optimized bias current of 30 mA (~1.5Ith) with corresponding extinction ratio (ER) of 6 dB and the external injection power of −9 dBm is (are) required for such a wavelength-locked universal transmitter to carry the 16-QAM and 122-subcarrier formatted OFDM and data-stream. By increasing external injection-locking from −9 dBm to 0 dBm, the peak-to-peak chirp of the OFDM data stream reduces from 7.7 to 5.4 GHz. The side mode suppression ratio (SMSR) of up to 50 dB is achieved with wider detuning range between −0.5 nm to 2.0 nm under an injection power of 0 dBm. By modulating such a colorless laser diode with an OFDM data stream of 122 subcarriers at a central carrier frequency of 1.5625 GHz and a total bandwidth of 3 GHz, the transmission data rate of up to 12 Gbit/s in standard single-mode fiber over 25 km is demonstrated to achieve an error vector magnitude (EVM) of 5.435%. Such a universal colorless DWDM-PON transmitter can deliver the optical OFDM data-stream at 12 Gbit/s QAM-OFDM data after 25-km transmission with a receiving power sensitivity of −7 dBm at BER of 3.6×10^{-7} when pre-amplifying the OFDM data by 5 dB.

OCIS codes: (140.3520) Lasers, injection-locked; (060.4080) Modulation; (060.2330) Fiber optics communications.

References and links

1. J. Prat, C. Arellano, V. Polo, and C. Bock, "Optical network unit based on a bidirectional reflective semiconductor optical amplifier for fiber-to-the-home networks," IEEE Photon. Technol. Lett. **17**(1), 250–252 (2005).
2. W. R. Lee, M. Y. Park, S. H. Cho, J. Lee, C. Kim, G. Jeong, and B. W. Kim, "Bidirectional WDM-PON based on gain-saturated reflective semiconductor optical amplifiers," IEEE Photon. Technol. Lett. **17**(11), 2460–2462 (2005).
3. H.-D. Kim, S.-G. Kang, and C.-H. Lee, "A low-cost WDM source with an ASE injected Fabry-Perot semiconductor laser," IEEE Photon. Technol. Lett. **12**(8), 1067–1069 (2000).
4. W. Hofmann, E. Wong, G. Bohm, M. Ortsiefer, N. H. Zhu, and M. C. Amann, "1.55-μm VCSEL arrays for high-bandwidth WDM-PONs," IEEE Photon. Technol. Lett. **20**(4), 291–293 (2008).
5. A. Banerjee, Y. Park, F. Clarke, H. Song, S. Yang, G. Kramer, K. Kim, and B. Mukherjee, "Wavelength-division-multiplexed passive optical network (WDM-PON) technologies for broadband access: a review," J. Opt. Netw. **4**(11), 737–758 (2005).
6. Y.-H. Lin, C.-J. Lin, G.-C. Lin, and G.-R. Lin, "Saturated signal-to-noise ratio of up-stream WRC-FPLD transmitter injection-locked by down-stream data-erased ASE carrier," Opt. Express **19**(5), 4067–4075 (2011).

#188513 - $15.00 USD Received 9 Apr 2013; revised 4 May 2013; accepted 4 May 2013; published 5 Jul 2013

7. G.-R. Lin, Y.-S. Liao, Y.-C. Chi, H.-C. Kuo, G.-C. Lin, H.-L. Wang, and Y.-J. Chen, "Long-cavity Fabry–Perot laser amplifier transmitter with enhanced injection-locking bandwidth for WDM-PON Application," J. Lightwave Technol. **28**(20), 2925–2932 (2010).
8. K.-I. Suzuki, H. Masuda, S. Kawai, K. Aida, and K. Nakagawa, "Bidirectional 10-channel 2.5 Gbit/s WDM transmission over 250km using 76nm (1531-1607nm) gain-band bidirectional erbium-doped fibre amplifiers," Electron. Lett. **33**(23), 1967–1968 (1997).
9. G.-R. Lin, H.-L. Wang, G.-C. Lin, Y.-H. Huang, Y.-H. Lin, and T.-K. Cheng, "Comparison on injection-locked fabry–perot laser diode with front-facet reflectivity of 1% and 30% for optical data transmission in WDM-PON system," J. Lightwave Technol. **27**(14), 2779–2785 (2009).
10. S.-M. Lee, K.-M. Choi, S.-G. Mun, J.-H. Moon, and C.-H. Lee, "Dense WDM-PON based on wavelength locked Fabry-Perot laser diodes," IEEE Photon. Technol. Lett. **17**(7), 1579–1581 (2005).
11. Y. J. Wen and C. J. Chae, "WDM-PON upstream transmission using Fabry–Perot laser diodes externally injected by polarization-insensitive spectrum-sliced supercontinuum pulses," Opt. Commun. **260**(2), 691–695 (2006).
12. S.-Y. Lin, Y.-C. Chi, H.-L. Wang, G.-C. Lin, J.-W. Liaw, and G.-R. Lin, "Coherent injection-locking of long-cavity colorless laser diodes with low front-facet reflectance for DWDM-PON transmission," IEEE J. Sel. Top. Quantum Electron., **19**, (2013). (to be published)
13. Z. Xu, Y.-J. Wen, W.-D. Zhong, C.-J. Chae, X.-F. Cheng, Y. Wang, C. Lu, and J. Shankar, "High-speed WDM-PON using CW injection-locked Fabry-Pérot laser diodes," Opt. Express **15**(6), 2953–2962 (2007).
14. G.-R. Lin, T.-K. Chen, Y.-H. Lin, G.-C. Lin, and H.-L. Wang, "A weak-resonant-cavity Fabry–Perot laser diode with injection-locking mode number-dependent transmission and noise performances," J. Lightwave Technol. **28**(9), 1349–1355 (2010).
15. G.-R. Lin, T.-K. Cheng, Y.-H. Lin, G.-C. Lin, and H.-L. Wang, "Suppressing chirp and power penalty of channelized ASE injection-locked mode-number tunable weak-resonant-cavity FPLD transmitter," IEEE J. Quantum Electron. **45**(9), 1106–1113 (2009).
16. W. Shieh and C. Athaudage, "Coherent optical orthogonal frequency division multiplexing," Electron. Lett. **42**(10), 587–589 (2006).
17. W. Shieh, H. Bao, and Y. Tang, "Coherent optical OFDM: theory and design," Opt. Express **16**(2), 841–859 (2008).
18. J. M. Tang, P. M. Lane, and K. A. Shore, "High-speed transmission of adaptively modulated optical OFDM signals over multimode fibres using directly modulated DFBs," J. Lightwave Technol. **24**(1), 429–441 (2006).
19. J. Yu, M. F. Huang, D. Qian, and G.-K. Chang, "Centralized lightwave WDM-PON employing 16-QAM intensity modulated OFDM downstream and OOK modulated upstream signals," IEEE Photon. Technol. Lett. **20**(18), 1545–1547 (2008).
20. R.-P. Giddings, X.-Q. Jin, E. Hugues-Salas, E. Giacoumidis, J.-L. Wei, and J. M. Tang, "Experimental demonstration of a record high 11.25Gb/s real-time optical OFDM transceiver supporting 25km SMF end-to-end transmission in simple IMDD systems," Opt. Express **18**(6), 5541–5555 (2010).
21. C.-W. Chow, C. H. Yeh, C. H. Wang, F. Y. Shih, and S. Chi, "Signal remodulation of OFDM-QAM for long reach carrier distributed passive optical networks," IEEE Photon. Technol. Lett. **21**(11), 715–717 (2009).
22. C.-W. Chow, C.-H. Yeh, C.-H. Wang, F.-Y. Shih, C.-L. Pan, and S. Chi, "WDM extended reach passive optical networks using OFDM-QAM," Opt. Express **16**(16), 12096–12101 (2008).
23. W.-R. Peng, J. Chen, and S. Chi, "On the phase noise impact in direct-detection optical OFDM transmission," IEEE Photon. Technol. Lett. **22**(9), 649–651 (2010).
24. J. L. Wei, X. Q. Jin, and J. M. Tang, "The influence of directly modulated DFB lasers on the transmission performance of carrier-suppressed single-sideband optical OFDM signals over IMDD SMF systems," J. Lightwave Technol. **27**(13), 2412–2419 (2009).
25. W.-J. Jiang, C.-T. Lin, A. Ng'oma, P.-T. Shih, J. Chen, M. Sauer, F. Annunziata, and S. Chi, "Simple 14-Gb/s short-range radio-over-fiber system employing a single-electrode MZM for 60-GHz wireless applications," J. Lightwave Technol. **28**(16), 2238–2246 (2010).
26. C.-T. Lin, J. Chen, P.-T. Shih, W.-J. Jiang, and S. Chi, "Ultra-high data-rate 60 GHz radio-over-fiber systems employing optical frequency multiplication and OFDM formats," J. Lightwave Technol. **28**(16), 2296–2306 (2010).
27. C.-T. Lin, Y.-M. Lin, J. J. Chen, S.-P. Dai, P. T. Shih, P.-C. Peng, and S. Chi, "Optical direct-detection OFDM signal generation for radio-over-fiber link using frequency doubling scheme with carrier suppression," Opt. Express **16**(9), 6056–6063 (2008).
28. G.-R. Lin, Y.-C. Chi, Y.-C. Li, and J. Chen, "Using a L-Band Weak-Resonant-Cavity FPLD for subcarrier amplitude pre-leveled 16-QAM-OFDM transmission at 20 Gbit/s," J. Lightwave Technol. **31**(7), 1079–1087 (2013).
29. J. L. Wei, A. Hamié, R. P. Giddings, and J. M. Tang, "Semiconductor optical amplifier-enabled intensity modulation of adaptively modulated optical OFDM signals in SMF-based IMDD systems," J. Lightwave Technol. **27**(16), 3678–3688 (2009).
30. Y.-C. Chi, Y.-C. Li, H.-Y. Wang, P.-C. Peng, H.-H. Lu, and G.-R. Lin, "Optical 16-QAM-52-OFDM transmission at 4 Gbit/s by directly modulating a coherently injection-locked colorless laser diode," Opt. Express **20**(18), 20071–20077 (2012).

#188513 - $15.00 USD Received 9 Apr 2013; revised 4 May 2013; accepted 4 May 2013; published 5 Jul 2013

31. Y.-C. Chi, Y.-C. Li, and G.-R. Lin, "Specific jacket SMA-connected TO-can package FPLD transmitter with direct modulation bandwidth beyond 6 GHz for 256-QAM single or multisubcarrier OOFDM up to 15 Gb/s," J. Lightwave Technol. **31**(1), 28–35 (2013).
32. R. Lang, "Injection locking properties of a semiconductor laser," IEEE J. Quantum Electron. **18**(6), 976–983 (1982).
33. F. Mogensen, H. Olesen, and G. Jacobsen, "Locking conditions and stability properties for a semiconductor lasers with external light injection," IEEE J. Quantum Electron. **21**(7), 784–793 (1985).
34. A. Murakami, K. Kawashima, and K. Atsuki, "Cavity Resonance Shift and Bandwidth Enhancement in Semiconductor Lasers with Strong Light Injection," IEEE J. Quantum Electron. **39**(10), 1196–1204 (2003).
35. L. A. Coldren and S. W. Corzine, "*Diode Lasers and Photonic Integrated Circuits*," (Wiley, New York, 1997).
36. C.-C. Lin, Y.-C. Chi, H.-C. Kuo, P.-C. Peng, C. J. Chang-Hasnain, and G.-R. Lin, "Beyond-bandwidth electrical pulse modulation of a TO-can packaged VCSEL for 10 Gbit/s injection-locked NRZ-to-RZ transmission," J. Lightwave Technol. **29**(6), 830–841 (2011).
37. K. Kikuchi and T. Okoshi, "Measurement of FM noise, AM noise, and field spectra of 1.3 μm InGaAsP DFB lasers and determination of the linewidth enhancement factor," IEEE J. Quantum Electron **21**(11), 1814–1818 (1985).
38. C. H. Henry, "Theory of the linewidth of semiconductor lasers," IEEE J. Quantum Electron. **18**(2), 259–264 (1982).
39. Y.-H. Lin, G.-C. Lin, H.-L. Wang, Y.-C. Chi, and G.-R. Lin, "Compromised extinction and signal-to-noise ratios of weak-resonant-cavity laser diode transmitter injected by channelized and amplitude squeezed spontaneous-emission," Opt. Express **18**(5), 4457–4468 (2010).
40. G.-R. Lin, Y.-C. Chi, Y.-S. Liao, H.-C. Kuo, Z.-W. Liao, H.-L. Wang, and G.-C. Lin, "A pulsated weak-resonant-cavity laser diode with transient wavelength scanning and tracking for injection-locked RZ transmission," Opt. Express **20**(13), 13622–13635 (2012).
41. L. Hanzo, W. Webb, and T. Keller, *Single- and Multi-Carrier Quadrature Amplitude Modulation –Principles and Applications for Personal Communications, WLANS and Broadcasting* (John Wiley & Sons, Ltd, 2000).

1. Introduction

High bit-rate optical transmission system in fiber-optic communication network will be needed with the rapid growth on delivering high-quality audio and video data in the near future. The dense wavelength division multiplex passive optical network (WDM-PON) is currently considered to be a promising solution for next-generation high-capacity passive optical access network. Since early years, the spectrally sliced and wavelength injection-locked transmitters including semiconductor optical amplifiers (SOAs) [1,2] and Fabry-Perot laser diodes (FPLDs) [3] have emerged as alternative approaches to replace the typical candidates such as distributed feedback laser diodes (DFBLDs), vertical-cavity surface-emitting lasers (VCSELs) [4], and external-cavity controlled wavelength tunable lasers (TLs) [5] for the dense wavelength-division-multiplexing (DWDM-PON) applications. The major limitation of DWDM-PON is the preset channel spacing ranged between 50 and 200 GHz that may deviate from the specified wavelength of the single-mode transmitter source. The general single-mode lasers such as DFBLDs or VESCLs are hard to meet the demand of DWDM wavelength selection flexibility during the operation in the DWDM-PON network. The tolerance and instability of manufacture process usually introduces additional wavelength inaccuracy and the on-line discrimination needs to be accomplished after package. Recently, the relatively weak resonant cavity (WRC) Fabry-Perot laser diode (FPLD) was made to meet the requirements of the unified transmitters for DWDM-PON systems, which exhibits a broadband gain spectrum with tiny longitudinal modes to support different wavelength channels via the external photon injection technique. By employing low-reflective coating on the front-facet reflectance of a FPLD to form a weakly resonant cavity [6,7], a cost-effective colorless laser diode [8] operated under directly on-off-key modulation with a non-return-to-zero (NRZ) data-stream at 2.5-Gbit/s has recently emerged as a novel universal DWDM-PON transmitter after injection-locking. Such a 600-μm long cavity FPLD exhibits very weak longitudinal modes within a relatively broadband gain spectral linewidth, which can be easily wavelength injection-locked via non-coherent [9–11] or coherent [12] light sources for multiple or single mode carrier generation with accompanied enhancement on its direct-modulation bandwidth [13]. Without sacrificing the broadband gain spectrum as compared to the conventional SOAs, the output coherence of such a weak-resonant-cavity FPLD under

#188513 - $15.00 USD Received 9 Apr 2013; revised 4 May 2013; accepted 4 May 2013; published 5 Jul 2013

wavelength injection-locking is significantly improved [3]. This is attributed to the relatively low injection power budget originated from the extremely low front-facet reflectance. This is mainly attributed to the specific design on the released injection-locking range of the weak longitudinal modes, which further suppress the spontaneous emission noise [14] added to the background state of output when setting the direct modulation at off-level. Besides, the chirp suppression and noise reduction of such a long-cavity colorless laser diode [15] with its finite end-facet reflectance set between SOA and FPLD is particularly suitable for noise-insensitive modulation.

Recently, the optical orthogonal frequency-division multiplexing (OFDM) format has also been considered to fuse with the DWDM-PON system as a new class of encoding format due to its spectral usage efficiency for transmitters with limited frequency bandwidth [16]. The fusion of OFDM and DWDM-PON provides a potential subscriber network with both higher channel capacity and more format flexibility for the fiber-to-the-home applications. Another benefit of the OFDM is its immunity to the inter-symbol interference during long-haul transmission through the use of cyclic pre□x (CP) [16–18]. Nowadays, many efforts have been paid on applying the OFDM format in the last-mile, short- and long-haul DWDM-PON transmissions. Based on an externally modulated DFBLD, Yu and coworkers [19] have demonstrated a 16-QAM-OFDM transmission at 10-Gbit/s over 25-km long distance with a bit-error-ratio (BER) as low as 5×10^{-4}. Giddings *et al.* [20] have made a milestone work on 64-QAM OFDM-PON with a BER of 1×10^{-3} at a total bit rate of 11.25 Gbit/s based on a directly modulated DFBLD. In addition, some remarkable achievements of OFDM-PON were also reported by research peers, such as the use of signal re-modulation to build up up- and down-stream QAM-OFDM channels for a long-reach bi-directional WDM-PON [21,22]. Besides, the phase impact [23] and directly modulated laser performance [24] in a direct-detection optical OFDM transmission system have been discussed. Later on, the radio-over-fiber (RoF) distribution technology becomes a promising option for extending the reachable distance of wireless microwave signals, by taking the advantage of extremely large signal bandwidth and extremely low loss in fibers [25]. A novel RoF based 10 Gbit/s OFDM transmission system that seamlessly integrates the 60-GHz millimeter-wave carrier with the DWDM-PON transmission system was reported by Lin *et al.* [26], which utilized the carrier suppression technique to implement a high-capacity and frequency-doubled transmission with negligible penalty of sensitivity in SMF over 50 km [27]. In particular, some new pre-scaling or adaptive modulation [28,29] techniques for the OFDM data-stream have also been proposed to modify the formats and power of the original OFDM data-stream carried by different OFDM subcarriers.

More recently, the back-to-back optical OFDM transmission with the aforementioned long-cavity colorless WRC-FPLD under coherent injection and direct modulation [30] has preliminarily emerged to achieve a total bit-rate as high as 20 Gbit/s [28,31]. When comparing to the ordinary multiple mode laser FPLD, the WRC-FPLD with long cavity (>600 μm) and weak end-facet reflection (<1%) is designed to increase the mode density and to facilitate the injection-locking efficiency. At same injection-locking condition, the side-mode suppressing ratio (SMSR) of the WRC-FPLD is easier to exceed over that of a typical multi-mode FPLD, withstanding the long-distant transmission induced chromatic dispersion in standard single-mode fiber. In view of these enhanced performances, the WRC-FPLD indeed presents intriguing features as being a new class of universal DWDM-PON transmitter candidate; however, the long-distant optical OFDM transmission performance of the long-cavity colorless WRC-FPLD based WDM-PON system has never been discussed. In this work, the parametric optimization on coherent injection-locking and direct OFDM modulation of WRC-FPLD is demonstrated to carry the 16 QAM-OFDM data-stream at a total bit-rate of 12 Gbit/s for DWDM-PON transmission in standard single-mode fiber (SMF) over 25 km. The effects of dynamic frequency chirp, on/off extinction ratio (ER), and side-mode suppression ratio (SMSR) on the improvement of error vector magnitude (EVM) and bit error ratio (BER) are

#188513 - $15.00 USD Received 9 Apr 2013; revised 4 May 2013; accepted 4 May 2013; published 5 Jul 2013

elucidated. The trade-off among the injection-locking power, the microwave amplifier gain and the biased current of the injection-locked colorless WRC-FPLD is discussed to obtain highest SNR and lowest BER for comparing the back-to-back and 25-km OFDM-PON transmission performances.

2. Experimental setup

Figure 1 illustrates the testing bench of the coherently wavelength injection-locked colorless WRC-FPLD for the transmission of 16-QAM and 122-subcarrier OFDM data-stream at 12 Gbit/s in SMF over 25 km. The long-cavity colorless WRC-FPLD with a threshold of 17 mA is not a common FPLD, which is fabricated by dicing a conventional FPLD epitaxial wafer with a cavity length up to 600-μm, then coating the rear- and front-facet with the sputtered TiO_2/SiO_2 multilayer films corresponding reflectances of 99% and 1%, respectively. Such a weak resonant cavity design not only facilitates external optical injection efficiency but also preserves the partial coherence of the laser. In comparison with the typical FPLDs, the long-cavity colorless WRC-FPLD provides dense channel modes to fit the DWDM-PON applications. Under free-running condition, the WRC-FPLD exhibits a larger threshold current than that of a typical FPLD. When operating at twice the threshold condition, the output power of WRC-FPLD is about 0.3 dBm. The wavelength injection-locking of the colorless WRC-FPLD was achieved by a tunable laser with its power level changing from −12 to 0 dBm. This results in a single-mode carrier at a small injecting power budget. The OFDM data-stream was converted by an optical receiver (Nortel, pp-10G) after transmitting back-to-back or over 25-km long SMF. Figure 1 illustrates the testing bench for the 16-QAM-52-OFDM optical transmission at total bit rate of 4 Gbit/s by using a coherently injection-locked WRC-FPLD transmitter. The slave WRC-FPLD is injection-locked by single-mode wavelength-tunable laser for broadband tuning its wavelength.

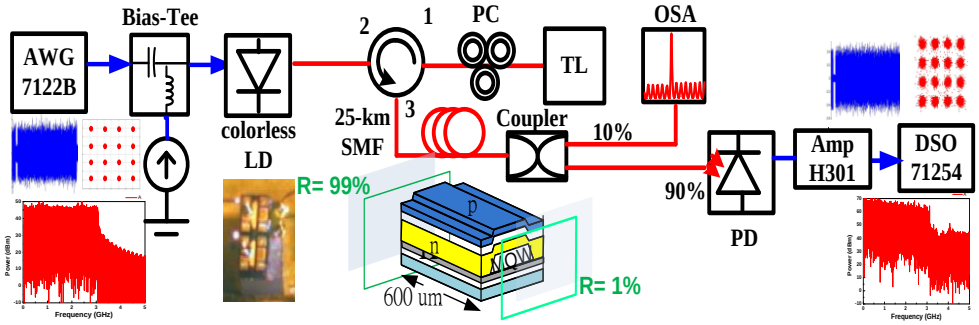

Fig. 1. The optical 16-QAM and 122-subcarrier OFDM testing bench for a directly modulated long-cavity colorless WRC-FPLD that is coherently injection-locked by tunable laser. Middle inset: the device configuration and the photograph of long-cavity colorless WRC-FPLD. AWG: arbitrary waveform generator, TL: tunable laser, OSA: optical spectrum analyzer, PD: photodetector, Amp: amplifier. DSO: digital signal oscilloscope.

The operating bandwidth, central frequency, and subcarrier number of OFDM were set as 3 GHz, 1.5625 GHz, and 122, respectively. The subcarrier frequency spacing was set as 24.4 MHz to protect the QAM data from severe distortion by the uneven frequency response of the testing bench. The designed electrical 16-QAM OFDM data with its waveform and corresponding spectrum shown in left part of Fig. 1 was delivered by an arbitrary waveform generator (Tektronix, AWG 7122B) with a sampling rate of 12.5 GS/s, which was employed to directly modulate the colorless WRC-FPLD DC biased at different currents via a bias-tee (Picosecond Pulse Lab, ZX85-12G-S+). The V_{pp} of the analog waveform FFT converted from the OFDM data was set as 0.7 volts. The injection-locking mode spectrum and SMSR were measured by optical spectrum analyzer (Advantest, Q8384). The electrical OFDM waveform was amplified by a microwave amplifier (JDSU, HC301) with variable gain between 0 and 26

#188513 - $15.00 USD Received 9 Apr 2013; revised 4 May 2013; accepted 4 May 2013; published 5 Jul 2013

dB before modulating the WRC-FPLD. The optoelectronic converted OFDM data at receiving end was captured by a real-time oscilloscope (Tektronix, DSO 71254) with a sampling rate of 200 GS/s. The decoded constellation plot of the received OFDM data delivered by the long-cavity colorless WRC-FPLD was analyzed, its EVM, SNR and BER were calculated via the computer program to compare with the origin constellation plot of the OFDM data stream.

3. Results and discussions

3.1 the injection-locking performance of the long-cavity colorless WRC-FPLD

The steady-state solutions of the following rate equations for a coherently injection-locked single-mode WRC-FPLD is derived to study the threshold current change can be written as [32,33]

$$\frac{dN(t)}{dt} = \frac{\eta_i I}{q} - \frac{N(t)}{\tau_s} - \Gamma \upsilon_g g'\left[N(t) - N_{tr}\right] S(t) \equiv 0, \tag{1}$$

$$\frac{dS(t)}{dt} = \frac{1}{2}\left\{\left[\Gamma \upsilon_g g'\left(N(t) - N_{tr}\right) - \frac{1}{\tau_p}\right]\right\} S(t) + \beta_{sp}\frac{N(t)}{\tau_s} + \kappa\sqrt{S_{inj}S(t)}\cos\phi(t) \equiv 0, \tag{2}$$

$$\frac{d\phi(t)}{dt} = \frac{\alpha}{2}\left\{\left[\Gamma \upsilon_g g'\left(N(t) - N_{tr}\right) - \frac{1}{\tau_p}\right]\right\} - \kappa\sqrt{\frac{S_{inj}}{S(t)}}\sin\phi(t) - \Delta\omega_{inj} \equiv 0, \tag{3}$$

where η_i denotes the internal quantum efficiency, I the bias current of WRC-FPLD, q the electronic charge, N the carrier number, τ_s the carrier life time, υ_g the group velocity, g' the differential gain coefficient ($g'=\delta g/\delta n$), $S(t)$ the photo number of slave laser, Γ the optical confinement factor N_{tr} the carrier number of slave laser under transparent condition, τ_p the photon life time, β_{sp} the spontaneous rate, κ the feedback coupling ratio, S_{inj} the injected photo number, α the linewidth enhancement factor, Δw_{inj} the detuning frequency, $\phi(t)$ denotes the phase difference between the internal and injected fields, as expressed by, $\phi(t)= \phi(t)-\Delta w_{inj}t-\phi_{inj,}$ where$\phi(t)$ and ϕ_{inj} are the phase of the injection-locked semiconductor laser and the constant phase of the injection-locked semiconductor laser output under external injection. Under a steady-state condition, the left-hand side of the Eqs. (1) and (2) are zero.

By substituting the time variable term $S(t)=S_s$ the photon number in the injection-locked mode at steady-state condition, and $\phi(t)= \phi_s$ the phase change in the injection-locked mode, we obtain [34]

$$\phi_s = \sin^{-1}\left(-\frac{\Delta\omega_{inj}}{\kappa\sqrt{1+\alpha^2}}\sqrt{\frac{S_s}{S_{inj}}}\right) - \tan^{-1}\alpha \equiv -\tan^{-1}\alpha. \tag{4}$$

By assuming $\Delta\omega_{inj}=0$ and ignoring the spontaneously emitted photons in our case. The summation of steady-state Eqs. (2) and (3) can be approximated as

$$\left[\Gamma \upsilon_g g'\left(N_s - N_{tr}\right) - \frac{1}{\tau_p}\right] = \frac{2\kappa}{\sqrt{1+\alpha^2}}\sqrt{\frac{S_{inj}}{S_s}}. \tag{5}$$

After injection-locking, the reduced carrier number difference can be applied into Eq. (5). Thus, the threshold current is decreased by injection-locking can be described by substituting Eq. (5) into Eq. (1),

#188513 - $15.00 USD Received 9 Apr 2013; revised 4 May 2013; accepted 4 May 2013; published 5 Jul 2013

$$I_{th}' \equiv I_{th} - I_{inj} = \frac{q}{\eta_i}\left[\left(\frac{N_s}{\tau_s} - \frac{S_s}{\tau_p}\right) - \frac{2\kappa}{\sqrt{1+\alpha^2}}\sqrt{S_{inj}S_s}\right], \tag{6}$$

where I_{th} is the threshold current, I_{inj} is the reduced threshold current caused by external photon injection. As a result, the output power of the WRC-FPLD can be derived as

$$P_{out} = \frac{\eta_0\eta_i h\nu}{q}\left(I - \frac{q}{\eta_i}\left[\left(\frac{N_s}{\tau_s} - \frac{S_s}{\tau_p}\right) - \frac{2\kappa}{\sqrt{1+\alpha^2}}\sqrt{S_{inj}S_s}\right]\right), \tag{7}$$

where $h\nu$ denotes the energy per photon, $\eta_0=[\alpha_m/(\alpha_m+\alpha_{int})]$ is with α_m and α_{int} denoting the facet loss and the internal loss, respectively. The Eq. (7) describes the single-mode output response of the WRC-FPLD with the aid of coherent injection-locking. In addition to the injection power, the feedback coupling ratio and the linewidth enhancement factor of the WRC-FPLD also play the contradictory effect to the output level after injection-locking. As a result, the basic properties of colorless WRC-FPLD biased at twice threshold current and injection-locked at different power levels are shown in Fig 2. Table 1 with detailed descriptions for all properties of WRC-FPLD under free-running or injection-locking cases is shown as below.

Table 1. Characteristic Parameters of WRC-FPLD

Type of property	Free-running	-9 dBm	-6 dBm	-3 dBm
Threshold current	17 mA	15 mA	13 mA	11 mA
RIN peak	5.1 GHz	5.5 GHz	6.5 GHz	7.5 GHz
RIN @ <5GHz	–94 dBc/Hz	–101 dBc/Hz	–101 dBc/Hz	–102 dBc/HZ
SMSR	0	40 dB	45 dB	50 dB
3-dB cutoff frequency	5.8 GHz	3.5 GHz	3.25 GHz	3.2 GHz
6-dB cutoff Frequency	6.4 GHz	7.25 GHz	7.2 GHz	4.3 GHz
Frequency Slope (dB/GHz)	–0.38	–1	–1.37	–1.38

#188513 - $15.00 USD Received 9 Apr 2013; revised 4 May 2013; accepted 4 May 2013; published 5 Jul 2013

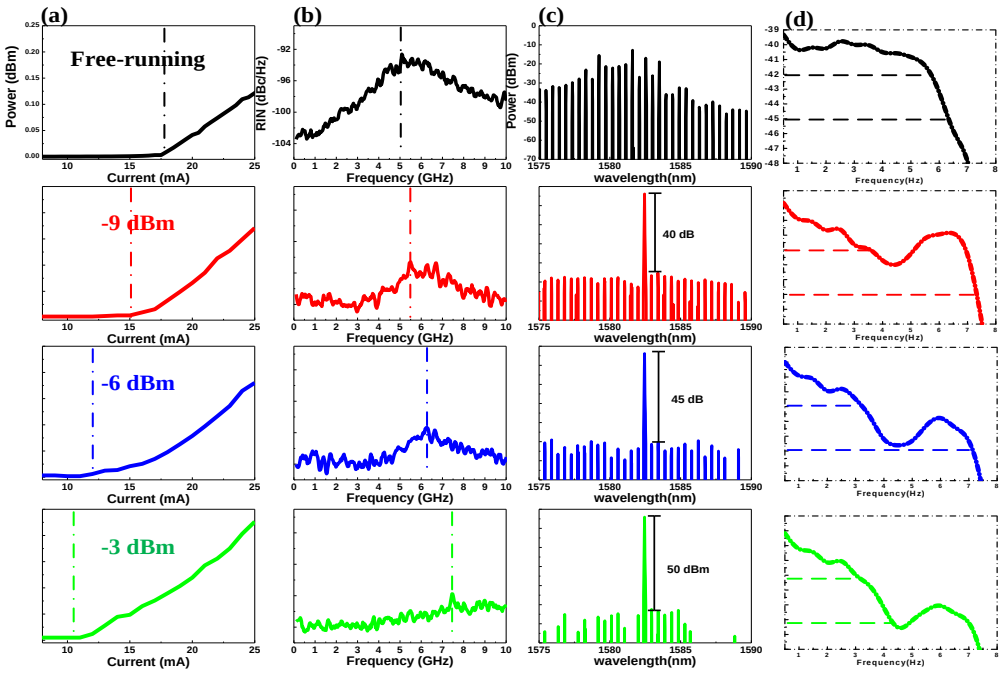

Fig. 2. (a) P-I curve, (b) relative intensity noise spectra, (c) optical spectra, (d) frequency responses of the long-cavity colorless WRC-FPLD free-running and injection-locked at different powers.

The P-I curves of the free-running and injection-locked WRC-FPLD are shown in Fig. 2(a), in which the threshold current is decreased with injection-locking power, as described by aforementioned formula. When comparing with the free-running case, the threshold current is reduced up to 5 mA with injection-locking power enlarged up to −3 dBm. Such a threshold current reduction effectively benefits from the direct OFDM modulation with a large amplitude. With an equivalent WRC-FPLD load resistance of 25 Ω, the 5-mA current increment corresponds to a peak voltage enlargement of $\Delta V_p = \Delta I_p \times R_L = 5 \times 25 = 125$ mV. This eventually leads to the improvement on both SNR and BER of the received OFDM data-stream under same biased condition of the WRC-FPLD. However, the frequency response of the colorless WRC-FPLD shown in Fig. 2(d) indicates a lower modulating throughput at higher injection powers. This causes the negative power-to-frequency slope ~~is~~ significantly enlarged by intense injection-locking. Figure 2(c) shows that the single-mode spectrum of the colorless WRC-FPLD after wavelength injection-locking the free-running WRC-FPLD. The dense multi-mode spectrum of the free-running colorless WRC-FPLD turns to be a coherently single-mode with SMSR of up to 40 dB even at an injection locking power as small as −9 dBm. The SMSR is further enhances by 10 dB with the injection power enlarging up to 0 dBm. Figures 2(b) compares the relative intensity noise spectra of the colorless WRC-FPLD at free-running and injection-locking cases. The relaxation oscillation related noise peak of the free-running WRC-FPLD is dramatically increased to −93 dBc/Hz at an offset frequency of 5 GHz or higher, which also indicates a smaller modulation bandwidth of the free-running colorless WRC-FPLD. After injection-locking, the colorless WRC-FPLD significantly reduces the relaxation oscillation noise power by 15-20 dB and enhances its peak frequency from 6 GHz to 8 GHz as the injection-locking power enlarges from −9 to −3 dBm. Theoretically, the relaxation oscillation frequency of the coherently injection-locked single-mode WRC-FPLD can be written as [35,36]

#188513 - $15.00 USD Received 9 Apr 2013; revised 4 May 2013; accepted 4 May 2013; published 5 Jul 2013

$$\omega_r = \sqrt{\frac{\Gamma v_g g'}{qV}\left\{ I - \frac{q}{\eta_i}\left[\left(\frac{N_s}{\tau_s} - \frac{S_s}{\tau_p}\right) - \frac{2\kappa}{\sqrt{1+\alpha^2}}\sqrt{S_{inj}S_s}\right]\right\}}, \tag{8}$$

where V is the active region. With the relaxation oscillation frequency, the relative intensity noise, RIN, of the WRC-FPLD can also be described as a function of the mode linewidth, the relaxation oscillation frequency, and the threshold current under single-mode coherent injection-locking case, as written by [37,38]

$$\begin{aligned} RIN &= \frac{16(\Delta\nu)_{ST}}{\omega_r^4 \tau_{\Delta N}^2} + \frac{2h\nu}{P_0}\left[\eta_0 \frac{I + I_{th}^{'}}{I - I_{th}^{'}} + (1-\eta_0)\right] \\ &= \frac{16\Gamma^2 v_g g n_{sp}}{V(\Gamma v_g \frac{g^{'}(I - I_{th}^{'})}{qV})^2 \tau_{\Delta N}^2} + \frac{2h\nu}{\frac{\eta_0 \eta_i h\nu}{q}(I - I_{th}^{'})}\left[\eta_0 \frac{I + I_{th}^{'}}{I - I_{th}^{'}} + (1-\eta_0)\right], \\ &= \frac{16 g n_{sp} V q^2}{v_g g^{'2}(I - I_{th}^{'})^2 \tau_{\Delta N}^2} + \frac{2}{\frac{\eta_i}{q}(I - I_{th}^{'})}\left[\frac{I + I_{th}^{'}}{I - I_{th}^{'}} + \frac{(1-\eta_0)}{\eta_0}\right] \\ &= \frac{1}{(I - I_{th}^{'})^2}\left\{\frac{16 g n_{sp} V q^2}{v_g g^{'2} \tau_{\Delta N}^2} + \frac{2q}{\eta_i}\left[\frac{(I - I_{th}^{'})}{\eta_0} + 2I_{th}^{'}\right]\right\} \end{aligned} \tag{9}$$

where n_{sp} is the population inversion factor, $\tau_{\Delta N}$ the differential carrier lifetime. Under coherent injection-locking, it is observed that the relaxation oscillation frequency is up-shifted with the external injection level, whereas the RIN power level exhibits a decreasing trend with the injection power, as obtained by substituting the Eq. (6) into the Eq. (9) [39]. Indeed, the coherent injection-locking facilitates the reduction on noise power at background and relaxation oscillation peak of RIN spectrum. Note that the high negative power-to-frequency slope results in the low 3-dB cutoff frequency of WRC-FPLD. It turns out that the WRC-FPLD exhibits an optimized injection-locking condition without sacrificing the modulating bandwidth. The compromised injection power is observed for obtaining the single-mode injection-locking with high SMSR and reducing the intensity noise by up-shifting the relaxation oscillation peak.

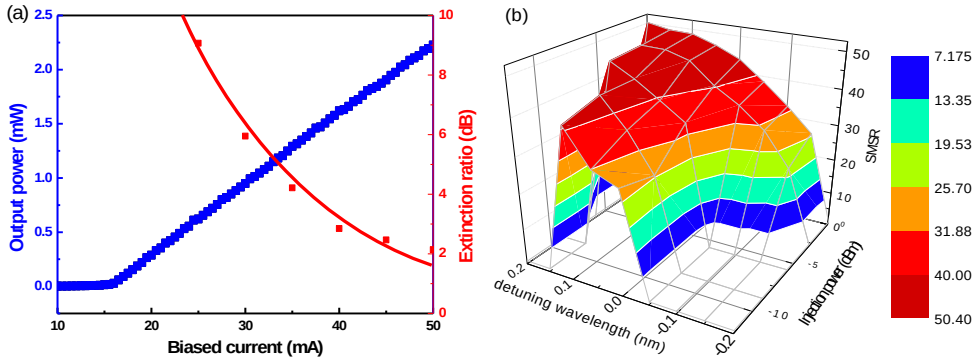

Fig. 3. (a) The extinction ratio of the received OFDM data-stream carried by the WRC-FPLD transmitter at different bias currents. (b) The 3D contour of SMSR for the injection-locked WRC-FPLD as a function of detuning wavelength and injection power.

Although the spontaneous emission noise is greatly attenuated by increasing bias current of WRC-FPLD, the extinction ratio (ER) of the optical OFDM data-stream with a constant V_{pp} in time domain conversely decreases accordingly. Figure 3(a) shows the ER (red line) of the received OFDM data-stream as a function of bias current, which is decreased from 10 to 2

#188513 - $15.00 USD Received 9 Apr 2013; revised 4 May 2013; accepted 4 May 2013; published 5 Jul 2013

dB when increasing the bias current of WRC-FPLD from 25 to 50 mA. Since the ER is defined as the ratio of maximum and minimum power of the transmitted optical OFDM data-stream, the higher ER induced by decreasing the bias current of the WRC-FPLD may suffer from a clipping effect due to the threshold lasing condition of the WRC-FPLD. To completely perform the OFDM waveform without distortion, the optimized ER is set as 4-6 dB by adjusting the bias current. Under continuous-wave injection, the unique low end-face reflectance feature of the WRC-FPLD effectively reduces the requirement of high-level injection for conventional FPLDs, and the relatively broadened linewidth of the original longitudinal mode facilitate the slave WRC-FPLD a wide injection-locking wavelength range [40]. The side-mode suppressing ratio (SMSR) is a function of both injection locking power and wavelength concurrently. To achieve a high SMSR of >40 dB shown in Fig. 3(b), the injecting wavelength of the tunable laser can be detuned away from the longitudinal mode of the slave WRC-FPLD, and the maximal tunable range between −0.5 nm to 2.0 nm under an injection power of 0 dBm. When decreasing the injection-locking power from 0 to −10 dBm, the injection-locking range of the WRC-FPLD significantly shrinks to ±0.05 nm. These results elucidate that both the injection-locking power and the end-face reflectance of the WRC-FPLD equally contribute to broadening the wavelength injection-locking range.

3.2 The back-to-back and 25-km-SMF transmitted 16-QAM OFDM data carried by the coherently wavelength injection-locked colorless WRC-FPLD

By using the injection-locked colorless WRC-FPLD at different powers and biased currents, the Fig. 4 shows the back-to-back BER performance of the OFDM data stream transmission at a total bit rate of 12 Gbit/s and a receiving power of 0 dBm. At same injection-locking level, the BER response reaches a minimum at biased current of 35-40 mA. When biasing the colorless WRC-FPLD at lower current near the threshold condition, the lower part of OFDM waveform is slightly clipped and contains a large spontaneous emission noise, which inevitably causes a large chirp on the directly OFDM modulated WRC-FPLD output with a high peak-to-average power ratio (PAPR). The chirp can be effectively suppressed but saturated with decreasing the external injection-locking power down to –9 dBm.

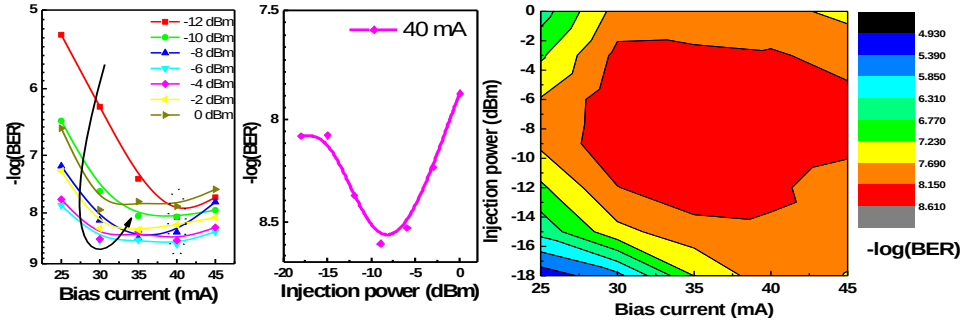

Fig. 4. The back-to-back BER of OFDM data transmitted with long-cavity colorless WRC-FPLD at different biased currents and injection-locking powers.

The impact of externally coherent injection-locking on chirp parameter of the pseudorandom binary sequence (PRBS) data stream is performed, which helps to evaluate the effect of chirp on the transmission performance of the WRC-FPLD carried OFDM data-stream, as shown in Fig. 5(a). To simulate the bandwidth of OFDM data in our test bench, the data rate of PRBS is set as 3 Gbit/s. By increasing external injection-locking from –9 dBm to 0 dBm, the peak-to-peak chirp of the OFDM data stream decreases from 7.7 to 5.4 GHz within 0.3 ns at a bias current of 35 mA (nearly $2I_{th}$ of the WRC-FPLD). As the threshold current is slightly decreased by external wavelength injection-locking, the ER of OFDM signal carried by WRC-FPLD transmitter is reduced accordingly. More important, although

#188513 - $15.00 USD Received 9 Apr 2013; revised 4 May 2013; accepted 4 May 2013; published 5 Jul 2013

the over injection could greatly improve the coherence and enlarge relaxation oscillation peak to higher frequency, which concurrently enlarges the negative power-to-frequency slope on the direct modulation response of such a long-cavity colorless WRC-FPLD. To simulate the SNR performance of the transmitted OFDM data-stream when suffering from the negative power-to-frequency slope, the original electrical OFDM data-stream has been pre-leveled with different negative slopes under back-to-back transmission. As a result, the BER as a function of negative power-to-frequency slope is shown in Fig. 5(b). By enlarging the injection-locking power from −9 to −3 dBm, the power-to-frequency slope of the direct modulation response for the WRC-FPLD is enlarged from −0.375 to −1.38 dB/GHz, as shown in the revised Fig. 2. The SNR is decreased by only 1 dB when enlarging the negative power-to-frequency slope form −3 to −5 dB/GHz. The theoretical BER is calculated by using $BER=0.375\times erfc(SNR/10)^{0.5}$ [41]. For the simulated direct modulation response of the WRC-FPLD with a negative power-to-frequency slope smaller than −7 dB/GHz, the simulated BER slightly increases from 2.5×10^{-10} to 5.03×10^{-5} when the SNR decreases from 18 dBm to 16 dBm under back-to-back transmission. The SNR significantly decays by 6 dB with enlarging the negative power-to-frequency slope from −7.5 dB/GHz to −9 dB/GHz, providing a serious degradation on the transmission BER from 3×10^{-3} to 0.148 accordingly. For the coherently injection-locked WRC-FPLD at a bias current of 40 mA, the SNR reduction induced with increasing negative power-to-frequency slope (from −0.38 to −1.38 dB/GHz) is only 0.5 dB by increasing the injection-locking level from −9 dBm to −3 dBm. This only degrades the BER from 2.5×10^{-9} to 1.3×10^{-8}.

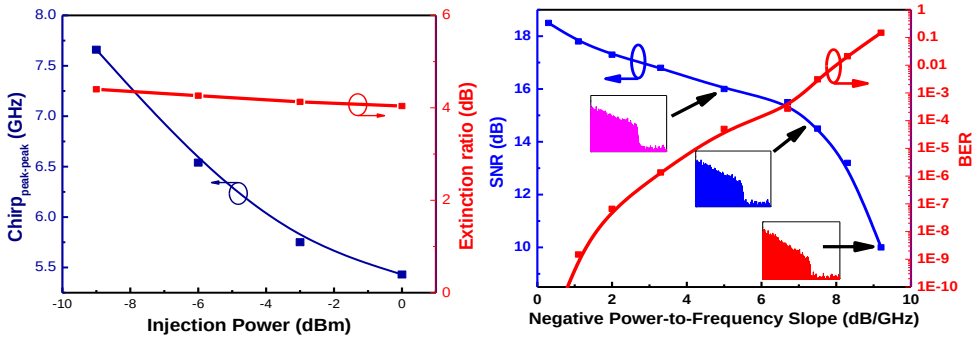

Fig. 5. (a) Peak-to-peak frequency chirp of the directly modulated WRC-FPLD with a PRBS pattern at 3 Gbit/s versus the external injection-locking power. (b) The SNR and BER performance as a function of the negative power-to-frequency slope of electrical OFDM data-stream.

The decrease of output OFDM power at higher subcarriers by over injection conversely degrades the OFDM data at same receiver sensitivity. These results indicate that the lowest BER of the received OFDM data at 3×10^{-9} can be obtained by operating the long-cavity colorless WRC-FPLD at DC bias and injection power of 35 mA and −9 dBm, respectively as observed from Fig. 4. For the free-running multi-mode WRC-FPLD, the significant distortion of the carried 16-QAM-OFDM data-stream is observed during 25-km transmission in SMF, which is attributed to the chromatic dispersion including the modal and fiber dispersions. Without injection-locking, the training symbol (TS) and cyclic prefix (CP) leading ahead the OFDM data-stream are absent after 25-km transmission, which results in an error on determining the data head and correcting the equalization. In contrast to the free-running case, the injection-locked WRC-FPLD shows very clear TS and CP in the received 16-QAM-OFDM data-stream with a better quality. The injection-locked WRC-FPLD easily gathers all the stimulated emission photons in a single mode, which therefore suppresses the mode-beating noise and chromatic dispersion during long-distant transmission. The received data-stream is less distorted with higher peak-to-peak amplitude, as shown in Fig. 6. The

#188513 - $15.00 USD Received 9 Apr 2013; revised 4 May 2013; accepted 4 May 2013; published 5 Jul 2013

demodulated constellation plot also reveals a good data quality after 25-km transmission with reducing EVM from 9.89% to 6.19% and improving BER from 9.01×10^{-2} to 4.2×10^{-5}, even with an injection power as low as −15 dBm.

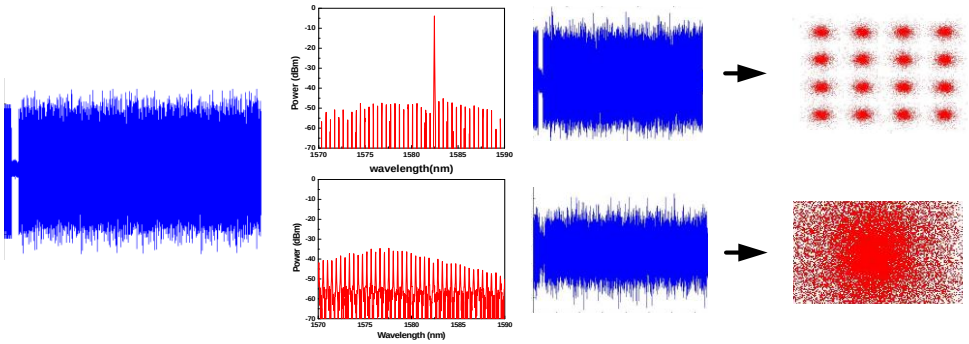

Fig. 6. Received 16-QAM-OFDM data-streams and decoded constellation plots from free-running (left) and injection-locked (right) WRC-FPLDs.

Figure 7 shows the corresponding BER performance of the 25-km transmitted 16-QAM-OFDM data-stream (without post amplification) carried by the single-mode injection-locked WRC-FPLD, which is obtained at a receiving power of −7 dBm with changing injection-locking powers and biased currents. At same injection-locking level, the BER response of WRC-FPLD renders an initial decline and a subsequent rising trend. In comparison with back-to-back BER performance shown in Fig. 4, a similar sagging behavior on the BER versus bias current is observed between 20 and 25 mA due to the waveform clipping around the threshold current of 20 mA. When the direct modulation is operated at nearly threshold condition, the improved BER is attributed to the reduced spontaneous emission noise with increasing bias current. However, the ER of OFDM data amplitude to noise amplitude turns out to be a dominant parameter on the BER response, as shown in Fig. 3(a). The lower ER at higher bias current also decreases the optical signal to noise ratio (OSNR). At an optimized bias around 30 mA, the best BER of $<10^{-4}$ for all injection levels can be observed. At a fixed current, the BER also reveals a reciprocal parabolic function with the injection-locking power, indicating a minimal error rate of 2.42×10^{-4} with the injection-locking power ranged between −6 to −12 dBm. The extremely low injection fails to meet the demand of power budget as well as SNR of the single-mode carrier, however; the extremely high injection could make the WRC-FPLD behave like a continuous-wave emitter with reduced frequency response and OSNR, as shown in Fig. 2(d). The injection-locking range was optimized between −6 and −12 dBm for a lowest BER of the 16-QAM-OFDM data carried by the directly modulated WRC-FPLD.

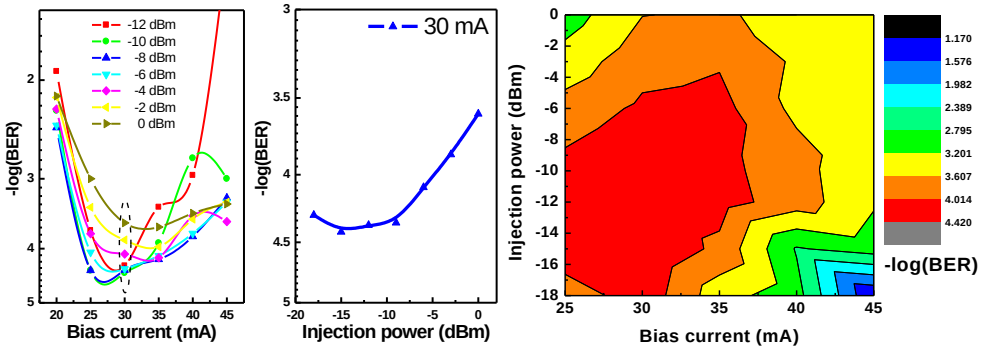

Fig. 7. The BER of received OFDM data after 25-km SMF transmission versus the bias currents and the injection-locking power.

#188513 - $15.00 USD Received 9 Apr 2013; revised 4 May 2013; accepted 4 May 2013; published 5 Jul 2013

After 25-km transmission, the optimized bias current and injection-locking power slightly decrease to 30 mA and −12 dBm for obtaining the least BER of 3.8×10^{-5} after 25-km transmission. In brief, the ER play a more important role than the spontaneous emission noise induced at lower bias and weaker injection-locking power during 25-km transmission. The OFDM data-stream suffers from a large dispersion and a power loss of up to 6 dB during transmission in SMF. To optimize the injection-locked WRC-FPLD for OFDM transmission over 25-km long SMF, the gain adjustment of a microwave amplifier after the AWG output is added to maximize the modulation depth. The 3-D BER contour of the 25-km transmitted 16-QAM and 122-subcarrier OFDM data-stream (with pre- and post- amplifications) carried by the single-mode injection-locked colorless WRC-FPLD is plotted as a function of bias current and amplifier gain is shown is Fig. 8. During analysis, the injection-locking power was set at −9 dBm to maintain the SMSR. The appropriate pre- and post-amplifications of OFDM waveform overcomes the noise figure from active components and conversion loss by photodetector. In particular, the surrounding area on the bottom of Fig. 8 with a relatively low microwave amplifier gain (< 1 dB) shows a worse BER than that of Fig. 7, which originates from the noise of electrical amplifier accompanied with the OFDM data under same condition.

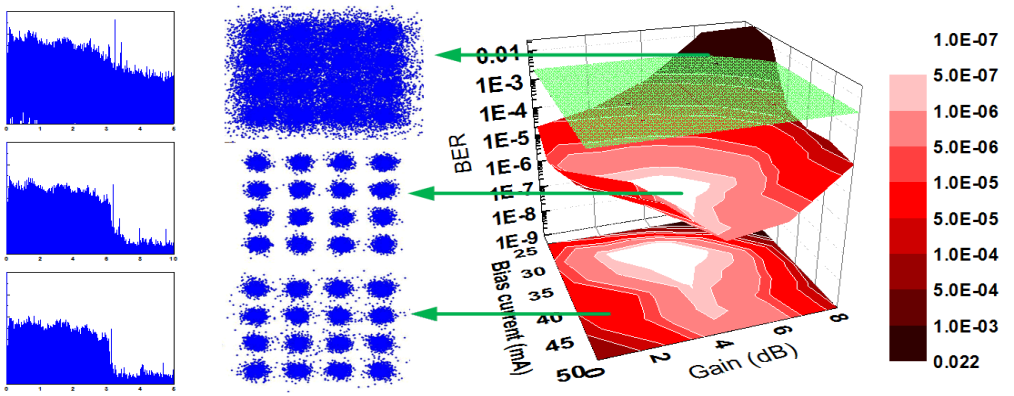

Fig. 8. Left: the worst and best normalized RF spectra (left) and constellation plots (middle) of the 16-QAM/122-subcarrier OFDM data carrier. Right: the 3-D BER contour (right) as a function of the gain of microwave amplifier and the bias current of the colorless WRC-FPLD.

The BER response reveals a significant reduction with the pre-amplifier gain increasing to 5±1 dB when biasing the WRC-FPLD at between 30 and 35 mA. With coherent injection at −9 dBm and bias at 30 mA for the WRC-FPLD, the BER improves from 3.8×10^{-5} to 2.2×10^{-7} and EVM reduces from 6.19% to 5.44% at a pre-amplifier gain of 5 dB. The OFDM data amplitude becomes too large as the pre-amplifier gain increases to 7±1 dB, which inevitably leads to the clipping of OFDM data and over modulation of the WRC-FPLD. This results in a huge distortion and frequency noise of the received OFDM data. The chirp induced damping modulation can be suppressed by elevating the bias current at a cost of reducing ER. An FEC criterion of BER=3.8×10^{-3} is shown in Fig. 8, which elucidates a large stability on the receiving performance of the 16-QAM OFDM data-stream carried by the coherently injection-locked WRC-FPLD with variously operating conditions under injection power of −9 dBm. The 3D contour of the received BER indicates a wide operation range for the bias current of the WRC-FPLD and the gain of the OFDM data amplifier to achieve the BER performance below the criterion of FEC.

4. Conclusion

The coherently injection-locked colorless weak-resonant-cavity Fabry-Perot laser diode under direct modulation is used for 16-QAM and 122 subcarrier optical OFDM transmission with a

#188513 - $15.00 USD Received 9 Apr 2013; revised 4 May 2013; accepted 4 May 2013; published 5 Jul 2013

maximal bit rate up to 12 Gbit/s at a carrier frequency of 1.5625 GHz. The largest SMSR of up to 50 dB is achieved when injection-locking the WRC-FPLD mode with wider detuning range between −0.5 nm to 2.0 nm under an injection power of 0 dBm. The threshold current is reduced up to 5 mA with injection-locking power with injection-locking power enlarged up to −3 dBm, which leads to the improvement on both SNR and BER of the received OFDM data-stream under same biased condition of the WRC-FPLD. Also, the WRC-FPLD significantly reduces the relaxation oscillation noise power by 20 dB and enhances its peak frequency 8 GHz with injection-locking power up to −3 dBm. Moreover, by increasing external injection-locking from −9 dBm to 0 dBm, the peak-to-peak chirp of the OFDM data stream reduces from 7.7 to 5.4 GHz. The constellation plot and real-time waveform of the optical 16-QAM-OFDM data carried by the WRC-FPLD at free-running and injection-locking cases are compared each other. Without injection, the WRC-FPLD carried OFDM data suffers from the SMF chromatic dispersion, which causes relatively large EVM and BER of up to 9.89% and 9.0×10^{-2}, respectively. The trade-off between injection power and bias current is considered for optimized BER of 25-km transmission is obtained. When the WRC-FPLD is biased at 30 mA and the moderate ER of OFDM data stream is 6 dB. Under low injecting power of −9 dBm, the optimized EVM and BER of the received optical OFDM data are greatly suppressed to 6.19% and 3.8×10^{-5}, respectively. Moreover, the trade-off between injection power, bias current and pre-amplifier gain has been discussed for the injection-locked WRC-FPLD based 16-QAM-OFDM transmission. When the pre-amplifier gain increasing up to 5 dB, the WRC-FPLD with injection-locking level at −9 dBm and bias at 30 mA, the BER improves from 3.8×10^{-5} to 2.2×10^{-7} and EVM reduces from 6.19% to 5.44%. As the pre-amplifier gain increases over 6 dB, the enlarged OFDM data amplitude leads to the clipping of OFDM data, and the high-speed waveform cannot be completed due to the excessive modulation depth induced chirp. The 3-D BER contour of the 25-km transmitted 16-QAM OFDM data-stream with pre-amplification carried by the injection-locked colorless WRC-FPLD shows a wider operating region under low BER condition.

Acknowledgments

This work was supported by the National Science Council of the Republic of China, Taiwan, under Contract 101-2221-E-002-071-MY3 and 100-2221-E-002-156-MY3.

#188513 - $15.00 USD Received 9 Apr 2013; revised 4 May 2013; accepted 4 May 2013; published 5 Jul 2013